# NITROGEN OXIDE TRACE GAS TRANSPORT AND TRANSFORMATION: II. MODEL SIMULATIONS COMPARED WITH DATA

Rodney T. Venterea[1] and Dennis E. Rolston[2]

The development of process-based models describing N oxide trace gas emissions from agricultural soils will assist in the assessment of present sources, prediction of future trends, and development of mitigation strategies. We compare the predictions of a transport and transformation model with data from intact soil core experiments and then use the model to evaluate the relative importance of individual processes after application of anhydrous ammonia to moderately acidic soil. Soil–gas concentrations of NO and $N_2O$ are adequately described using previously obtained kinetic expressions. Net NO surface fluxes are shown to be the result of high rates of subsurface gross NO production ($>100$ mg N m$^{-2}$ h$^{-1}$) balanced by gross consumption rates equivalent to 92–97% of gross production. The overall temperature dependency of NO emissions is described adequately as the net result of individual temperature-dependent processes. Denitrification was estimated to contribute only 8–14% of the total $N_2O$ source under primarily aerobic conditions, with the balance caused by abiotic nitrous acid decomposition. The bulk soil reactivity of $NO_2$ was estimated to be at least 500 times greater than the reactivity of NO. The potential for nonbiological nitrate formation is examined, and the effectiveness of pH control and subsurface fertilizer injection for minimizing gas losses are evaluated. (Soil Science 2002;167:49–61)

Key words: Nitric oxide, nitrous oxide, nitrite, modeling, trace gases.

**T**HE development of process-based models describing nitrogen (N) oxide emissions from soils has been identified as an important research need. Improved models will help to reduce uncertainties in global assessments of the importance of soils as sources of N oxide gases and will assist in the development of management strategies for minimizing gaseous N losses from agricultural systems (Mosier, et al., 1996; Matson, 1997). Several models have been developed that predict N oxide emissions from fertilized soils (Mosier, et al., 1983; Galbally and Johansson, 1989; Li, et al.,

[1]Institute of Ecosystem Studies, Box AB, Millbrook, New York 12545. Dr Venterea is corresponding author. E-mail: venterear@ecostudies.org

[2]Department of Land, Air and Water Resources, One Shields Avenue, University of California, Davis, California, 95616.

1992; Parton, et al., 1996; Grant, et al., 1993a; Riley and Matson, 2000; Venterea and Rolston, 2000b). Some of these models account for the diffusive flux of gaseous N species through the soil profile and predict surface efflux based on gradients across the soil–atmosphere interface. Although several existing models have been compared with field emissions data (Galbally and Johansson, 1989; Grant, et al., 1993b; Riley and Matson, 2000; Venterea and Rolston, 2000b), there have been few attempts to compare measured soil–gas concentrations with model predictions. Rudolph and Conrad (1996) and Rudolph et al. (1996) compared predictions of a steady-state diffusion–reaction model with soil-gas NO concentration profiles measured at 20-mm intervals in a 0.4-m-long column containing sieved and repacked acidic forest soil. Zero-order, spatially uniform NO production and first-order NO consumption kinetics were assumed, with parameters obtained from separate experiments

with the same soil. Hosen et al., (2000) compared steady-state models describing NO and $N_2O$ diffusion, production, and consumption with concentration profiles measured at 50-mm intervals in experimental lysimeter plots over a depth of 0.3 m. Zero-order, spatially uniform production was assumed over a finite production zone with Michaelis-Menten consumption kinetics occurring throughout the profile. Kinetic parameter values were obtained by fitting model output to observed depth profiles. In these modeling exercises, the kinetic expressions were not proposed to represent any specific microbial or chemical process, nor were they assumed to have functional dependence on soil variables such as inorganic N levels, soil pH, water content, or aerobic status although it is generally assumed that the underlying processes will be influenced by these variables.

In the present study, we compare measured soil-gas N oxide concentrations at 20-mm-depth intervals in 0.10-m intact core experiments described previously (Venterea and Rolston, 2002) with those predicted by a model that accounts for diffusive transport and kinetically controlled gas production and transformation (Venterea and Rolston, 2000b). Production of NO is assumed to occur because of abiotic decomposition of nitrous acid ($HNO_2$) (Venterea and Rolston, 2000a and c) with spatially-variable production rates determined from separately obtained kinetic coefficients and the distribution of soil pH and nitrite ($NO_2^-$) measured at 25-mm intervals in the same cores. Consumption of NO is caused by a first-order bulk soil consumption process and gas-phase oxidation by oxygen ($O_2$), which also results in the production of nitrogen dioxide ($NO_2$) gas. Production of $N_2O$ is caused by denitrification, as a function of soil anaerobic fraction, and also by $HNO_2$-mediated production. The model is used to analyze the relative importance of the assumed production and consumption processes under acidic conditions accompanied by $NO_2^-$ accumulation following anhydrous ammonia (AA) application. Rates of gross NO production are compared with previously estimated nitrification rates. The overall temperature dependency of net NO emissions is evaluated with respect to activation energies of individual component processes using previously obtained kinetic data. The importance of reactions involving the transformation of NO and $NO_2$ are evaluated. The model is used to examine the effectiveness of pH control and subsurface fertilizer injection for minimizing gaseous losses, and limitations of the current model are evaluated.

## MODELING APPROACH

The approach utilized here is based, in part, on a more comprehensive model describing nitrification biomass and substrate kinetics, and N oxide gas production, transport, and transformation under transient conditions (Venterea and Rolston, 2000b). In the present case, steady-state conditions are assumed based on evaluation of the measured N oxide gas concentrations in intact cores presented previously (Venterea and Rolston, 2002). The observed rates of change of measured NO and $N_2O$ concentrations at each sampling depth, which are approximations of the time derivatives in the transient transport equations (Venterea and Rolston, 2000b), were <2% of either the diffusion or reaction terms in these equations. An analysis based on that presented by Whitaker (1988) indicated that the quasi-steady state assumption was justified, particularly during the intermediate sampling times. Therefore, the system, comprised of three gas species (NO, $N_2O$, and $NO_2$), was described by diffusion-reaction equations in the form given by

$$-\frac{d}{dz}\left(D_{s,i}(z)\frac{dC_i}{dz}\right) = P_i(z) - S_i(z) \qquad (1)$$

where $i$ is the component index (NO, $i = 1$; $N_2O$, $i = 2$; $NO_2$, $i = 3$), $C_i$ is the gas-phase concentration (mg N $m^{-3}$) of component $i$, $P_i$ is the gross production rate (mg $m^{-3}$ soil $h^{-1}$), $S_i$ is the gross sink (consumption/transformation) rate (mg $m^{-3}$ soil $h^{-1}$), $z$ is soil depth (m), and $D_{s,i}$ is the soil gas diffusion coefficient ($m^3$ $m^{-1}$ soil $h^{-1}$). Values of the soil gas diffusion coefficient were calculated using the Buckingham-Burdine-Campbell (BBC) equation (Moldrup, et al., 1999), with the Campbell soil-water retention parameter (b) estimated using empirical functions as described previously (Venterea and Rolston, 2002). The sensitivity of simulation results to different empirical b estimates was examined. Regression functions describing water content ($\theta$, $m^3$ $H_2O$ $m^{-3}$ soil) and measured soil bulk density values ($\rho$, kg $m^{-3}$) previously obtained were used to calculate total soil porosity ($\phi$, $m^3$ pores $m^{-3}$ soil) and volumetric soil-air content ($\epsilon$, $m^3$ gas $m^{-3}$ soil), which were then used to calculate $D_{s,i}$ as a continuous function of $z$ using the BBC model. The gross production and consumption/transformation rates, $P_i$ and $S_i$, respectively, were based on previously developed kinetic models and data (Venterea and Rolston, 2000a, b, and c). Previously obtained regression functions describing soil pH, $NO_2^-$ concentra-

tions and water content as continuous functions of depth corresponding to each set of soil-gas concentration measurements were used as inputs to the kinetic expressions ($P_i$ and $S_i$) in Eq. (1). This approach was compared with simulations that assumed that $NO_2^-$ and pH levels were uniform across each 25-mm depth and equal to levels measured in homogenized samples from each depth. Kinetic expressions for $P_i$ and $S_i$ are described below for NO, $N_2O$ and $NO_2$, and parameter values in the kinetic terms are listed in Table 1.

### Nitric Oxide

Gross production of NO is described by

$$P_1 = \rho k_{P_{NO}} HNO_2 (z) \qquad (2)$$

where $\rho$ is the soil bulk density (kg m$^{-3}$) and $k_{P_{NO}}$ is a kinetic parameter representing the proportionality between the nitrous acid concentration ($HNO_2$, mg N kg$^{-1}$) and gross NO production as a result of abiotic $HNO_2$ decomposition (Venterea and Rolston, 2000a and c). For each core and sampling time, $HNO_2$ concentration was calculated as a function of $z$ using the obtained regression functions for $NO_2^-$ and soil pH, together with the pKa (3.3) for $HNO_2$ (Venterea and Rolston, 2002). Gross consumption of NO is described by

$$S_1 = \rho \, k_c C_1 - \epsilon \, (z) \, k_g O_2 \, (z) C_1^2 \qquad (3)$$

where $k_c$ is the first-order NO consumption rate coefficient (Remde, et al., 1989) representing the sum of all biological and chemical reactions occurring in the soil solid and liquid phases. The second term describes the chemical oxidation of NO by molecular oxygen ($O_2$) in the gas phase according to the elementary termolecular reaction

$$2 \, NO + O_2 \rightarrow 2 \, NO_2 \qquad (4)$$

with second-order dependency on NO ($C_1$) and first-order dependency on $O_2$ concentration. Kinetics for Reaction 4 are available in the atmospheric chemistry literature (Atkinson, et al., 1997). Air-filled porosity ($\epsilon$) and $O_2$ concentrations are calculated as a function of $z$ using previous results (Venterea and Rolston, 2002).

The effects of soil temperature on net NO flux were modeled using published activation energy ($E_a$) values for $k_{P_{NO}}$ (Venterea and Rolston, 2000c) and $k_g$ (Atkinson, et al., 1997) in Arrhenius expressions (Pauling, 1970) describing the individual temperature responses of $HNO_2$-mediated NO production and gas-phase NO oxidation, respectively, and a semiempirical model (Bird, et al., 1960) was used to describe the temperature dependency of NO gas diffusivity. Since activation energy data for bulk soil NO consumption in this soil are not available, $Q_{10}$ factors of 1.75, 2.0 and 2.25 were applied to the best-fit $k_c$ value found in the present model comparisons. The overall temperature dependency of predicted net NO emissions from the intact soil cores was evaluated at these different $Q_{10}$ factors and then compared with field data collected during the experiment described previously (Venterea and Rolston, 2000c). These data represent field NO fluxes and corresponding soil temperatures (averaged over the 0–0.10-m depth) measured at four locations within the field on a single day at 06:00 and 10:00 AM, and 4:00 PM local time.

TABLE 1

Kinetic parameters used in model simulations

| Parameter | Value |
|---|---|
| $k_{P_{NO}}$, NO production rate coefficient[†] | $3.4 \times 10^3$ g NO-N kg HNO$_2$-N$^{-1}$ h$^{-1}$ |
| $k_c$, NO consumption rate coefficient[§] | $2.0 \times 10^{-2}$ m$^3$ gas kg soil$^{-1}$ h$^{-1}$ |
| $k_g$, NO gas-phase oxidation coefficient[¶] | $1.37 \times 10^{-1}$ kg N$^{-1}$ m$^3$ gas ppm O$_2^{-1}$ h$^{-1}$ |
| $k_{P_{N2O}}$, N$_2$O production rate coefficient[¥] | 18–49 g N$_2$O-N kg HNO$_2$-N$^{-1}$ h$^{-1}$ |
| $P_d$, denitrified N$_2$O production rate[#] | f ($\Phi$) $\mu$g N$_2$O-N kg soil$^{-1}$ h$^{-1}$ |
| $k_s$, NO$_2$ consumption rate coefficient[‡] | $>10$ m$^3$ gas kg soil$^{-1}$ h$^{-1}$ |

[†]From linear analysis of kinetic data in Venterea and Rolston (2000b).
[§]From optimization of model output vs. data (Fig. 1).
[¶]Atkinson, et al. (1997).
[¥]From optimization of model output vs. data (Fig. 2).
[#]Linear interpolation of data in Table 2, as function of anaerobic fraction ($\Phi$).
[‡]Minimum estimated value based on stimulation results (Fig. 3).

### Nitrous Oxide

Most other models of denitrification-driven trace gas emissions would predict negligible $N_2O$ production under conditions of water-filled porosity $\leq 40\%$ (Cores A and B) or $\leq 50\%$ (Core C) and anaerobic fractions ($\Phi$) of $\leq 10^{-9}$ $m^3$ anaerobic fraction $m^{-3}$ soil in soils of medium texture (e.g., Li, et al., 1992; Parton, et al., 1996; Riley and Matson, 2000). One objective of the present evaluation was to estimate the relative contribution of denitrification, however small, to the intact core data using kinetic data measured in separate soil samples from the same field having similar water content and $NO_3^-$ levels, as described previously (Venterea and Rolston, 2000c). These data showed a small but increasing rate of $N_2O$ production with increasing water-filled porosity over the range of 20 to 60% in the absence of nitrification or $HNO_2$-mediated production in a composite containing 110 mg $NO_3^-$-N $kg^{-1}$ soil at pH 5.0. Therefore, two sources of $N_2O$ production were considered as given by

$$P_2 = \rho \left[ P_d \left( \Phi \left( z \right) \right) + k_{P_{N_2O}} HNO_2(z) \right]. \quad (5)$$

The denitrification-driven $N_2O$ production rate ($P_d$) was represented either as a function of water-filled porosity or $\Phi$, in the latter case by linear interpolation of data shown in Table 2, with nearly identical results. The second term in Eq. (5) is the $N_2O$ production rate attributable to abiotic $HNO_2$ decomposition, analogous to NO production, as previously described and measured (Venterea and Rolston, 2000c). Because of the extremely low anaerobic fractions and the lack of kinetic data for $N_2O$ transformation under such conditions, it was assumed that $N_2O$ reduction to dinitrogen ($N_2$) was negligible and, therefore, no $N_2O$ sink term was considered.

### Nitrogen Dioxide

The production of $NO_2$ occurs according to Eq. (4) and is, therefore, represented by an expression identical to the gas-phase NO sink term in Eq. (3) given by

$$P_3 = \epsilon \left( z \right) k_g \, O_2 \left( z \right) C_1^2. \quad (6)$$

Although transformations of $NO_2$ in soil and aqueous systems are known to occur (Reuss and Smith, 1965), the kinetics of the underlying reactions are not available. Here, first-order transformation is assumed, analogous to that for NO, given by

$$S_3 = \rho \, k_s \, C_3. \quad (7)$$

### Numerical Methods

The three differential equations represented by Eq. (1) with the above kinetic terms were solved numerically using finite difference algorithms with 1-mm spatial discretization and Newton-Raphson iteration with convergence criteria of $10^{-5}$ mg N $m^{-3}$. Predicted surface fluxes were calculated using Fick's equation and the gradient obtained from predicted concentrations at $z = 0$ and $z = 1$ mm. Algorithms were validated by verifying the equivalence of predicted fluxes with spatially integrated gross production and consumption rates within 2% deviation. Zero flux (Neumann type) boundary conditions (BCs) were applied at the lower boundary, and measured concentrations were used for upper (Dirichlet) BCs. For each simulation, the NO solution was first obtained and then applied in the $NO_2$ solutions. The model was applied to intermediate sampling times for Cores A, B, and C since the assumption of steady-state conditions was found to be most valid for these data. Additional analysis was done to evaluate gross production rates ($P_{I,i}$ mg N $m^{-2}$ $h^{-1}$) integrated over the entire length ($L = 0.10$ m) of the core, defined by

$$P_{I,i} = \int_0^L P_i(z) \, dz. \quad (8)$$

Integrals were calculated numerically using the model algorithms. It follows from Eq. (1) and (8)

TABLE 2
Kinetic data for denitrification-derived $N_2O$ production[†]

| Water-filled porosity $m^3$ $H_2O$ $m^{-3}$ pores | Anaerobic fraction[‡] ($\Phi$) $m^3$ anaerobic soil $m^{-3}$ soil | $N_2O$ production rate ($P_d$) μg N $kg^{-1}$ soil $h^{-1}$ |
|---|---|---|
| 0.20 | $2.85 \times 10^{-131}$ | 0.51 |
| 0.40 | $6.38 \times 10^{-16}$ | 1.46 |
| 0.60 | $2.10 \times 10^{-3}$ | 5.26 |

[†]Water-filled porosity and $P_d$ data are from Venterea and Rolston (2000b).
[‡]Calculated using method and parameters in Venterea and Rolston (2002).

that the difference between $P_{I,i}$ and the predicted surface flux is equal to the integrated consumption rate, $S_{I,i}$, defined analogously according to Eq. (8). Individual production and consumption terms in Eqs. (2–7) were also integrated over the core so that the relative importance of individual processes could be evaluated.

### Soil pH and Fertilizer Depth Effects

Additional simulations were performed to examine the potential for mitigating NO and $N_2O$ fluxes by (a) increasing the soil pH and (b) increasing the depth of fertilizer application. The soil pH values input to the model were increased above measured values at each soil depth over the range of 0 to 1 pH unit, corresponding to decreases in $HNO_2$ concentrations of 0 to 10-fold. In separate simulations, the depth of the fertilizer zone was increased over the range of 0 to 30 mm, by assuming a corresponding increase in thickness of an unfertilized soil layer above the 0.10 m deep fertilized zone. Within the upper layer, $NO_2^-$ levels were assumed to be $<0.01$ mg N $kg^{-1}$ so that $HNO_2$-mediated production was negligible, whereas all other processes were assumed to proceed.

### RESULTS

Numerical solutions of Eq. (1) for each species yielded steady-state concentration profiles and gas fluxes that were compared with measured data.

### Nitric Oxide Soil-Gas Profiles and Fluxes

Repeated simulations were done using Eq. (1) ($i = 1$) with varying $k_c$ values within the range of measured values reported previously (0.013–0.044 $m^3$ gas kg soil $h^{-1}$) (Venterea and Rolston, 2000c). The degree of deviation from measured NO soil-gas concentrations was evaluated by the root-mean-square error (RMSE) index (Moldrup, et al., 1997). The best-fit $k_c$ value was found to be 0.020 $m^3$ gas kg soil $h^{-1}$, with a minimal RMSE of 21 mg N $m^{-3}$ (34% of mean concentration) over all three cores. Predicted versus observed NO concentration profiles and individual RMSE values are shown in Fig. 1. The magnitude and spatial patterns in NO concentrations are predicted fairly well using a single $k_c$ value near the middle of the range of measured values, providing some validation to the modeling approach. Sensitivity analysis indicated that varying $k_c$ over the range of measured values had a significant impact on predicted surface fluxes (Table 3). Integrated gross NO production rates calculated by the model were ~10–50 times greater than predicted fluxes, and integrated gross consumption rates were equivalent to 92–97% of gross production (with $k_c = 0.020$). This demonstrates the importance of gross consumption, together with production, in controlling net NO surface fluxes. Oxidation of NO by $O_2$ in the gas-phase accounted for a small fraction (1.6–2.7%) of total integrated consumption. The model did not predict concentration profiles accurately in the upper 20 mm (Fig. 1), and, therefore, the predicted surface fluxes deviated by factors of 0.25 to 0.62 (underestimated) compared with measured fluxes.

### Nitrous Oxide Soil Gas Profiles and Fluxes

Simulations performed assuming denitrification to be the only source of $N_2O$ production ($k_{P_{N2O}}$-0) predict $N_2O$ soil-gas concentrations and fluxes much lower than observed (Fig. 2 and Table 4). Considering $HNO_2$-mediated production kinetics, the model predicts concentration profiles similar to those observed and also predicts that denitrification will account for only 8 to 14% of the total production when $HNO_2$-mediated production is considered. In most cases, predicted fluxes corresponding to each profile agreed fairly well with measured fluxes (Table 4). The $k_{P_{N2O}}$ values were optimized to each individual core and input data set, with a minimal RMSE of 3.1 mg N $m^{-3}$ (17% of mean concentration) over all three cores (individual RMSE values are shown in Fig. 2). The best-fit $k_{P_{N2O}}$ values obtained (18–49 g $N_2O$-N kg $HNO_2$-$N^{-1}$ $h^{-1}$) are similar to the range of values (20–44) measured previously in composite soil samples taken from the same field (Venterea and Rolston, 2000c). The higher $k_{P_{N2O}}$ values required to match the Core C data could indicate that the slightly higher anaerobic microsite fractions in Core C ($\sim 10^{-9}$ $m^3$ anaerobic soil $m^{-3}$ soil), compared with Cores A and B ($\leq 10^{-10}$), contributed to additional sources of $N_2O$, including the biological reduction of abiotically produced NO (Venterea and Rolston, 2000c), which were not accounted for in the present model. In order for denitrification alone to account for the observed data, the production parameter ($P_d$) would need to be increased 10 to 20 times above the values shown in Table 2. It should also be noted that the $P_d$ values assumed by the model (Table 2) are significantly higher than values obtained with another soil composite from the site (Venterea and Rolston, 2000c) and are also more than 30% higher than $N_2O$ production rates measured in silt loam soil at similar water contents under bulk aerobic conditions in previous studies

**(a) Core A**

RMSE = 22 (32 %)

○   day 10 data
.........   day 10 model
▲   day 16 data
——   day 16 model

**(b) Core B**

RMSE = 13 (27 %)

○   day 10 data
.........   day 10 model
▲   day 17 data
——   day 17 model

**(c) Core C**

RMSE = 26 (38 %)

○   day 15 data
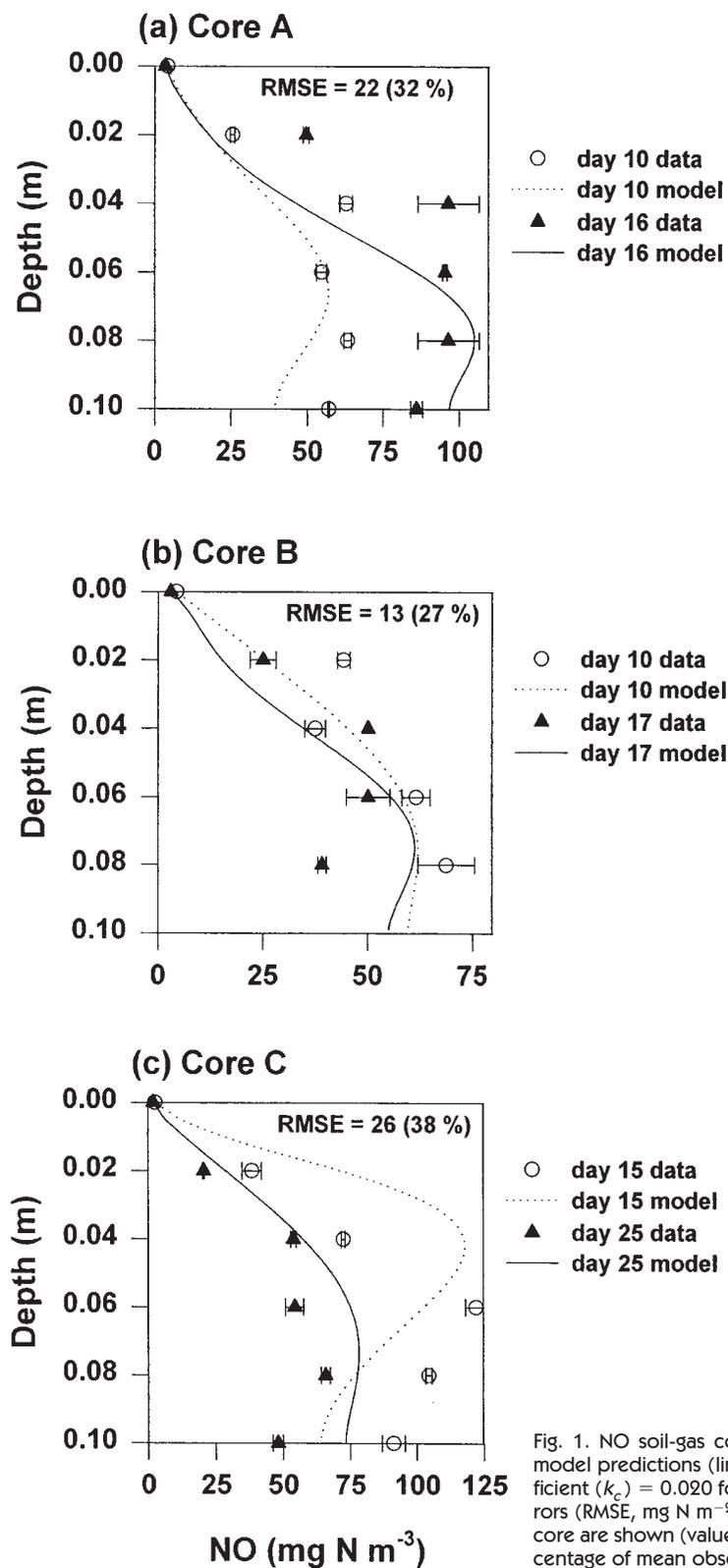.........   day 15 model
▲   day 25 data
——   day 25 model

Fig. 1. NO soil-gas concentration data (symbols) and model predictions (lines) using NO consumption coefficient ($k_c$) = 0.020 for all cases. Root-mean-square errors (RMSE, mg N m$^{-2}$ h$^{-1}$) of the predictions for each core are shown (values in parentheses are RMSE as percentage of mean observed concentration).

TABLE 3

Nitric oxide predicted and measured fluxes and integrated production rates

| | | mg N m$^{-2}$ h$^{-1}$ | | | |
|---|---|---|---|---|---|
| | $k_c = 0.013$ | Predicted NO flux[†] $k_c = 0.020$ | $k_c = 0.044$ | Measured NO flux | $P_{I,\,i}$[‡] |
| Core A–Day 10 | 12.9 | 5.5 (6.7) | 4.5 | 23.4 | 107 |
| Core A–Day 16 | 13.6 | 5.4 (7.0) | 3.5 | 23.5 | 174 |
| Core B–Day 10 | 14.9 | 9.7 (11.4) | 3.0 | 21.9 | 133 |
| Core B–Day 17 | 11.9 | 8.1 (6.6) | 3.6 | 18.9 | 116 |
| Core C–Day 15 | 24.3 | 16.3 (16.9) | 6.0 | 14.9 | 224 |
| Core C–Day 25 | 11.9 | 7.9 (19.3) | 3.2 | 12.7 | 150 |

[†]Simulated NO flux at varying values of $k_c$, NO consumption rate coefficient, m$^3$ gas kg soil$^{-1}$ h$^{-1}$. Values in parentheses for $k_c = 0.020$ are simulated fluxes assuming uniform NO$_2^-$ and pH levels across each 25 mm-depth.
[‡]Integrated gross production rate ($P_{I,1}$). $P_{I,1}$ minus predicted flux is integrated gross consumption rate ($S_{I,i}$).

(Goodroad and Keeney, 1983). Thus, the present modeling approach may be conservative with respect to the relative importance of sources other than denitrification.

The predictions of NO and N$_2$O flux were, in some cases, improved by assuming uniform distributions of NO$_2^-$ and soil pH across each 25-mm depth instead of continuous polynomial functions, although this was neither significant nor consistent (Tables 3–4). This assumption also did not significantly alter the resulting concentration profiles over the entire core depth (not shown) or change the best-fit $k_c$ or $k_{PN2O}$ values by more than 5%. Varying the b value in the BBC soil gas diffusion coefficient model over the range estimated by three different empirical relationships (Venterea and Rolston, 2002) had only minimal effects on the deviation of observed versus predicted fluxes or on any of the simulation results. Predicted fluxes were changed by 3.2 to 6.5%, and the RMSEs obtained in arriving at best-fit values of $k_c$ and $k_{PN2O}$ were changed by <0.1 and 4%, respectively, by varying b over the range of 5.0 to 6.2. The results shown in Figs. 1–2 are based on b values calculated from Eq. (12) in Moldrup et al. (1996) under the assumption that it is more accurate than other available estimates based on its consideration of bulk density as well as soil texture.

### Nitrogen Dioxide

Using the steady-state solution for NO with the input data for Core B, Day 10, and varying $k_s$ values, the model predicts steady-state NO$_2$ fluxes and soil–gas concentrations shown in Fig. 3 (results using input data from other sampling dates were similar). Thus, while the gas-phase reaction is not predicted to have a great effect on NO consumption and surface fluxes under these conditions, this process would be expected to result in significant levels of NO$_2$. Since the measured NO$_2$ soil–gas concentrations and fluxes were below detectable levels in all cases (<2 mg N m$^{-3}$ and <0.1 mg N m$^{-2}$ h$^{-1}$, respectively (Venterea and Rolston, 2002)), this implies a minimum value for the NO$_2$ gross transformation rate coefficient ($k_s$) of 10 m$^3$ gas kg soil$^{-1}$ h$^{-1}$. Thus, the overall reactivity of NO$_2$ within the soil matrix seems to be more than 500 times that of NO, based on the $k_s/k_c$ ratio.

### Temperature Effects on NO Flux

Assuming Q$_{10}$ factors of 1.75, 2.0, and 2.25 for the bulk soil NO consumption process described by the $k_c$ parameter, the model predicts an increase in net NO emissions with increasing soil temperature (Fig. 4a). Higher Q$_{10}$ factors resulted in greater NO consumption with increased temperature but were not sufficient to balance fully the increased HNO$_2$-mediated NO production and gaseous diffusion rates. Overall apparent E$_a$ values relating net NO emissions to soil temperatures were calculated, as is commonly done in NO field emissions studies (e.g., Williams, et al., 1987; Skiba, et al., 1992). Overall E$_a$ values predicted by the model (Fig. 4a) and calculated from field data (Fig. 4b) were similar. These results indicate that the overall E$_a$ values observed in the field (21 - 41 kJ mol$^{-1}$) can be explained in mechanistic terms as the net result of individual processes, each having different temperature sensitivities. Thus, the overall temperature sensitivity of net emissions is somewhat less than that which would be predicted based solely on the activation energy for HNO$_2$-mediated NO production (67 kJ mol$^{-1}$) in this soil (Venterea and Rolston, 2000c).
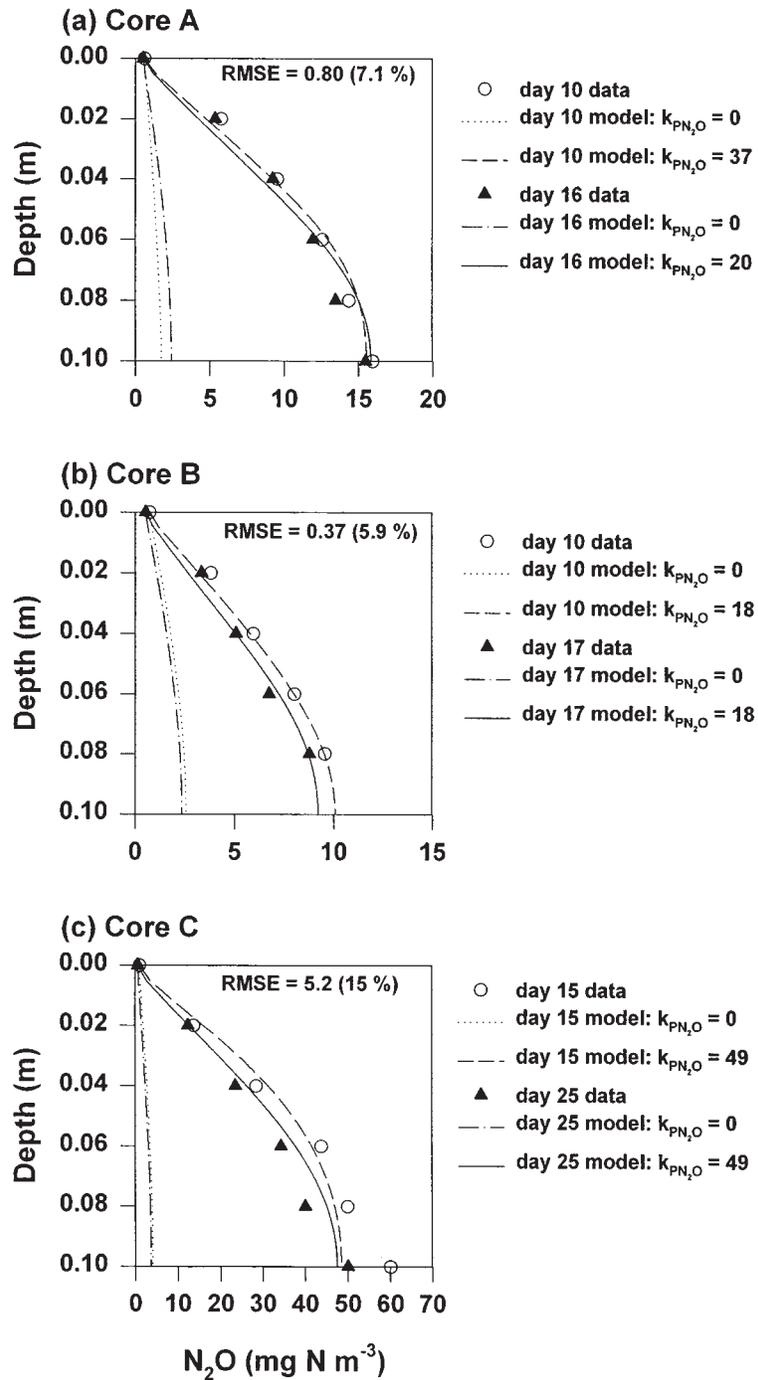
Fig. 2. $N_2O$ soil-gas concentration data (symbols) and model predictions (lines) using varying values of $N_2O$ production rate coefficient ($k_{PN2O}$). Root-mean-square errors (RMSE, mg N m$^{-2}$ h$^{-1}$) of the predictions for each core are shown (values in parentheses are RMSE as percentage of mean observed concentration).

TABLE 4

Nitrous oxide predicted and measured fluxes and integrated production rates[†]

| | mg N m$^{-2}$ h$^{-1}$ | | |
| | Integrated production rates and predicted flux due to | | |
| | Denitrification | Denitrification + HNO$_2$ decomposition[‡] | Measured flux |
| --- | --- | --- | --- |
| Core A–Day 10 | 0.09 | 1.3 (1.3) | 1.4 |
| Core A–Day 16 | 0.09 | 1.1 (1.1) | 1.1 |
| Core B–Day 10 | 0.10 | 0.80 (0.82) | 0.81 |
| Core B–Day 17 | 0.10 | 0.71 (0.68) | 1.8 |
| Core C–Day 15 | 0.18 | 2.9 (2.5) | 2.3 |
| Core C–Day 25 | 0.18 | 2.0 (2.6) | 2.0 |

[†]For steady-state system with no sinks, predicted surface flux is equivalent to integrated production rate.

[‡]Values in parentheses are simulated fluxes assuming uniform NO$_2^-$ and pH levels across each 25 mm–depth.

### Soil pH and Injection Depth Effects

Increasing soil pH by 1 unit above measured values reduced the predicted fluxes of NO and N$_2$O by 100% and 78%, respectively (Fig. 5). The NO flux had higher sensitivity because HNO$_2$ decomposition is the primary source mechanism assumed for NO, whereas some N$_2$O is assumed to originate from denitrification as well. Increasing the depth of the layer above the fertilized zone as little as 30 mm resulted in a 97% reduction in predicted NO flux (Fig. 5), due to the rapid NO transformation kinetics that are assumed to prevail in unfertilized soil. Since no sink term is assumed for N$_2$O, the increased depth had negligible effects on predicted N$_2$O flux. These results
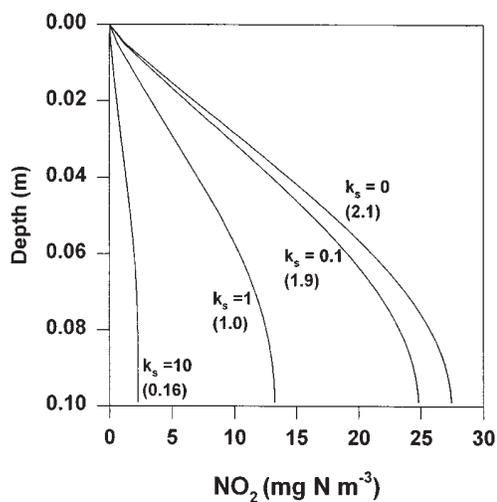
**(a) Model predictions of intact core NO flux**

Fig. 3. Predicted soil-gas concentrations and fluxes of NO$_2$ at varying values of NO$_2$ transformation coefficient ($k_s$). Predicted flux at each $k_s$ value is shown in parentheses (mg N m$^{-2}$ h$^{-1}$). Input data from Core B, Day 10.
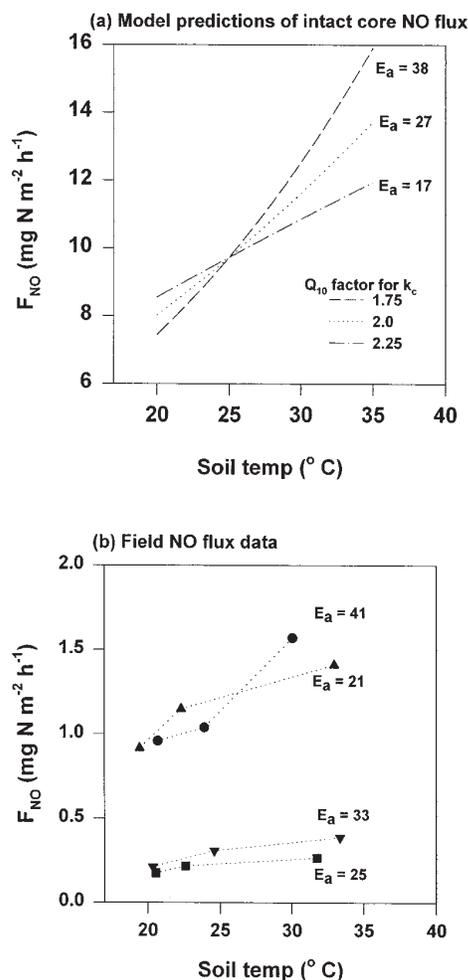
**(b) Field NO flux data**

Fig. 4. (a) Predicted temperature dependency of NO flux assuming varying Q$_{10}$ factors applied to NO consumption coefficient ($k_c$) using input data from Core B, Day 10, and (b) Measured NO fluxes vs average soil temperatures over 0–10 cm depth. E$_a$ values are overall apparent activation energy of net NO emissions.
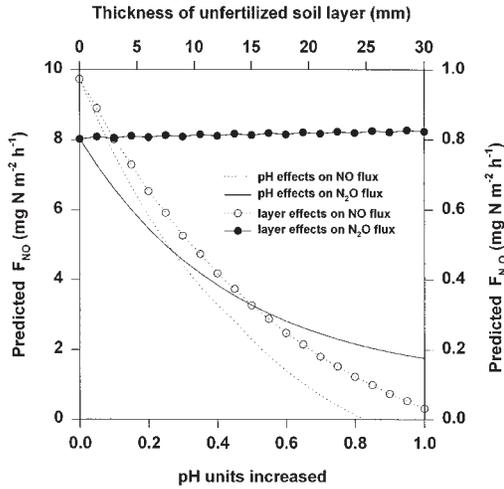
Fig. 5. Effects of increased pH and increased fertilizer depth on NO and $N_2O$ fluxes. Input data from Core B, Day 10.

imply that practical fertilizer management strategies may be very effective in minimizing N oxide gaseous losses.

## DISCUSSION

An interesting result of the integrated NO production analysis (Table 3) is that predicted gross production rates are 3 to 7 times higher than estimated net nitrification rates occurring in the cores (Venterea and Rolston, 2002). This result implies that there is significant recycling of NO back into the $NO_2^-$ pool as the NO diffuses through the profile and is subject to various transformations (Fig. 6). The $NO_2^-$ produced is then available for repeated transformation to NO. This is somewhat analogous to photochemical atmospheric reactions, whereby NO and

$NO_2$ can be recycled repeatedly between respective pools, depending on levels of $O_3$ and various organic radical species (Crutzen, 1981). In soil and aqueous systems, it is known that NO transformation can result directly in $NO_2^-$ as a result of chemical (Pires, et al., 1994) and/or biological oxidation processes (Freitag and Bock, 1990). The rapid transformation of $NO_2$ produced in the gas-phase suggested by the present modeling results would also be expected to result in $NO_2^-$ in the soil matrix as a result of $NO_2$ dissolution and subsequent chemical reactions (Reuss and Smith, 1965; Van Cleemput and Baert, 1984). These results, and the temperature-sensitivity analysis, provide further evidence of the importance of NO consumption processes in controlling net surface emissions. However, minimal data exist regarding the spatial and temporal dynamics of NO consumption kinetics, and there is limited understanding of biogeochemical controls over this process. For example, in multiple measurements of $k_c$ values made during soil incubation experiments with three agricultural soils similar in origin and composition to the present soil, high variabilities (CV = 50–70%) were noted, as was little correlation ($r^2 < 0.18$) with measured physical and chemical soil variables (Venterea and Rolston, 2000a).

The present analysis also implies that a significant fraction of the $NO_3^-$ produced may in fact have been the result of processes other than *Nitrobacter* oxidation of $NO_2^-$. Biological oxidation of NO (Koschorreck, et al., 1996) and chemical oxidation of $NO_2$ can result directly in $NO_3^-$ (Pauling, 1970). In addition, one of the proposed reactions for the aqueous disproportionation of $HNO_2$ itself results in $NO_3^-$ in a molar ratio of 2:1 with NO (Van Cleemput and Baert, 1976) as given by
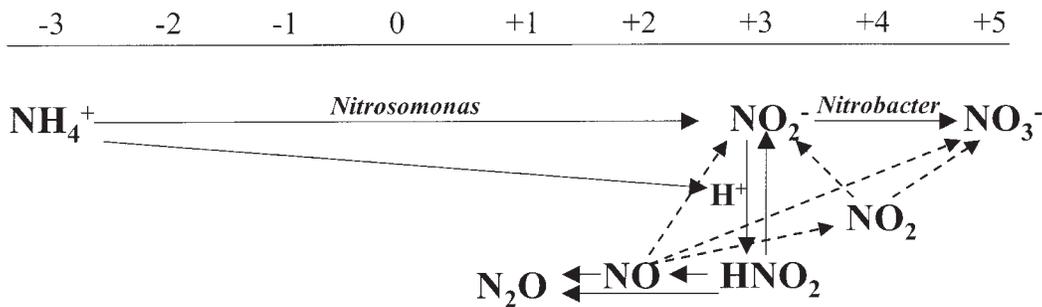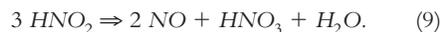


Fig. 6. N transformation pathways during nitrification under acidic conditions with $NO_2^-$ accumulation. Dashed lines indicate potential NO and $NO_2$ consumption pathways, including those described by Eqs. (4) and (11). Numbers across top refer to oxidation state of N in various forms shown below.

$$3 \ HNO_2 \Rightarrow 2 \ NO + HNO_3 + H_2O. \qquad (9)$$

Whereas another proposed abiotic reaction does not produce $NO_3^-$ directly, as given by

$$2 \ HNO_2 \Rightarrow NO + NO_2 + H_2O, \qquad (10)$$

the above reaction would subsequently be expected to result in $NO_3^-$ formation because of the chemical reaction (Van Cleemput and Baert, 1984) given by

$$2 \ NO_2 + H_2O \Rightarrow HNO_2 + HNO_3. \qquad (11)$$

The process of NO recycling through the $NO_2^-$ pool in acidic soil has been discussed previously with respect to the predominance of various processes occurring in closed incubation systems (Van Cleemput and Baert, 1984). The potential for nonbiological reactions contributing to $NO_3^-$ production in acid soils was first proposed by Reuss and Smith (1965) who studied the process in closed incubation systems with sterile soils. The present results indicate that recycling of NO and nonbiological $NO_3^-$ production may have been important in a biologically active system open to diffusive transport. Each time a molecule of NO passes through the sequence of potential pathways (Fig. 6), it may be partitioned into various end products including $NO_2^-$, $NO_3^-$, $NO_2$ or $N_2O$. Thus, these processes will influence the ratio of NO transformation products significantly and thereby impact N availability to plants and $NO_3^-$ leaching to groundwater. The gaseous diffusion of NO would be expected to play an important role in controlling the spatial distribution of end-products. Models such as the one described here may be useful in examining interactions between these processes when combined with additional kinetic information. For example, while the present simulations indicate that a 30-mm unfertilized layer may be effective in reducing NO fluxes (Fig. 5), the model does not consider the generation of $NO_2^-$ within the layer by the processes described above, which would tend to counteract the effectiveness of the strategy for minimizing NO emissions.

Results in Fig. 1 and Table 3 point out an important limitation of the current model of NO emissions. The overall best-fit $k_c$ value does not predict concentration profiles in the upper 20 mm adequately, and, therefore, the model generally underpredicted NO surface fluxes. Model assumptions regarding the distribution of pH and $NO_2^-$

over the upper 5–20 mm, which together drive $HNO_2$-mediated production, as well as the assumed spatially and temporally invariable $k_c$ value, may be responsible for much of this deviation. This points out the importance of both physical and biogeochemical processes occurring within very close proximity to the soil-atmosphere interface in determining surface trace gas fluxes. The generally closer agreement between predicted and observed $N_2O$ fluxes is likely caused by the more linear prevailing soil–gas $N_2O$ concentration gradients and less uncertainty regarding spatial uniformity of assumed parameters.

The $N_2O$ results provide strong evidence for the importance of $HNO_2$ decomposition as an important source of $N_2O$ emissions following AA applications. While this abiotic mechanism of $N_2O$ production has been addressed in earlier studies (Stevenson and Swaby, 1964; Bremner, et al., 1981), more recent considerations have downplayed the likelihood of $HNO_2$ contributing significantly to field emissions (Bremner, 1997). The present results are consistent with recent mechanistic studies (Thorn and Mikita, 2000) that have found direct spectroscopic evidence for chemical pathways mediating $N_2O$ formation via reaction of $HNO_2$ with phenolic soil organic matter constituents, and, therefore, suggest that abiotic reduction of $HNO_2$ may be a much more important source of $N_2O$ than generally assumed. Further work is required to understand better how soil organic matter may influence $N_2O$ production kinetics. For example, results of Thorn and Mikita (2000) suggest that differences in best-fit $(k_{PN_2O})$ values found between cores and sampling times in the present analysis (Fig. 2) may be attributable to variability in the concentration and/or composition of organic matter mediating the reactions with $HNO_2$.

CONCLUSIONS

The analysis presented here demonstrates how diffusion-reaction models can be implemented and evaluated by comparing predictions to experimental data. Model predictions agreed fairly well with observed NO and $N_2O$ soil–gas concentration profiles, allowing for several comparisons between individual processes and speculation regarding additional processes potentially important at the field scale. Some practical implications seem to follow. It is reasonable to assume, given what is known about the long-term acidifying effects of repeated application of AA and N fertilizers in general (Bouman, et al., 1995; Barak, et al., 1997), and the prevalence of AA use world-

wide, that conditions found in the present experiments may have broad applicability. Thus, the potential for high losses of $N_2O$ following AA application indicated here and in previous studies and summaries (Bremner, et al., 1981; Eichner, 1990) may be worth consideration by global emission assessment methodologies that presently do not consider such sources specifically (Mosier, et al., 1998). The relative ease and economic feasibility of pH modification and its effectiveness in reducing NO and $N_2O$ fluxes suggested by the present analysis may warrant recommendations for this practice as a means of mitigating N oxide trace gas losses from agricultural systems.

## ACKNOWLEDGMENTS

## REFERENCES

Atkinson, R., D. Baulch, R. Cox, R. F. Hampson, Jr., J. Kerr, M. Rossi, and J. Troe. 1997. Evaluated kinetic and photochemical data for atmospheric chemistry: Supplement VI. IUPAC subcommittee on gas kinetic data evaluation for atmospheric chemistry. Journal of Physical Chemical Reference Data. 26(6):1329–1499.

Barak, P., B. Jobe, A. Krueger, L. Peterson, and D. Laird. 1997. Effects of long-term soil acidification due to nitrogen fertilizer inputs in Wisconsin. Plant Soil 197:61–69.

Bird, R., W. Stewart, and E. Lightfoot. 1960. Transport Phenomena. John Wiley & Sons, New York.

Bouman, O., D. Curtin, C. Campbell, V. Biederbeck, and H. Ukrainetz. 1995. Soil acidification from long-term use of anhydrous ammonia and urea. Soil Sci. Soc. Am. J. 59: 1488–1494.

Bremner, J. 1997. Sources of nitrous oxide in soils. Nutr. Cycling Agroecosyst. 49:7–16.

Bremner, J., G. Breitenbeck, and A. Blackmer. 1981. Effect of anhydrous ammonia fertilization on emissions of nitrous oxide from soils. J. Environ. Qual. 10:77–80.

Crutzen, P. 1981. Atmospheric chemical processes of the oxides of nitrogen, including nitrous oxide. *In* Denitrification, Nitrification and Atmospheric $N_2O$. C. Delwiche (ed.). John Wiley & Sons Ltd., Chichester, UK, pp. 17–44.

Eichner, M. 1990. Nitrous oxide emissions from fertilized soils: Summary of available data. J. Environ. Qual. 19:272–280.

Freitag, A., and E. Bock. 1990. Energy conservation in *Nitrobacter*. FEMS Microbiol. Let. 66:157–162.

Galbally, I., and C. Johansson. 1989. A model relating laboratory measurements of rates of nitric oxide production and field measurements of nitric oxide emission from soils. J. Geophys. Res.-Atmos. 94(D5):6473–6480.

Goodroad, L., and D. Keeney. 1983. Nitrous oxide production in aerobic soils under varying pH, temperature and water content. Soil Biol. Biochem. 16: 39–43.

Grant, R., M. Nyborg, and J. Laidlaw. 1993a. Evolution of nitrous oxide from soil: I. Model development. Soil Sci. 156:259–265.

Grant, R., M. Nyborg, and J. Laidlaw. 1993b. Evolution of nitrous oxide from soil: II. Experimental results and model testing. Soil Sci. 156:266–277.

Hosen, Y., H. Tsuruta, and K. Minami. 2000. Effects of the depth of NO and $N_2O$ productions in soil on their emission rates to the atmosphere: Analysis by a simulation model. Nutr. Cycling Agroecosyst. 57:83–98.

Koschorreck, M., E. Moore, and R. Conrad. 1996. Oxidation of nitric oxide by a new heterotrophic *Pseudomonas sp*. Arch. Microbiol. 166:23–31.

Li, C., S. Frolking, and T. A. Frolking. 1992. A model of nitrous oxide evolution from soil driven by rainfall events: 1. Model structure and sensitivity. J. Geophys. Res.-Atmos. 97(D9):9759–9776.

Matson, P. 1997. $NO_x$ emission from soils and its consequences for the atmosphere and biosphere: critical gaps and research directions for the future. Nutr. Cycling Agroecosyst. 48:1–6.

Moldrup, P., C. Kruse, D. Rolston, and T. Yamaguchi. 1996. Modeling diffusion and reaction in soils: III. Predicting gas diffusivity from the Campbell soil-water retention model. Soil Sci. 161:366–375.

Moldrup, P., T. Olesen, D. Rolston, and T. Yamaguchi. 1997. Modeling diffusion and reaction in soils: VII. Predicting gas and ion diffusivity in undisturbed and sieved soils. Soil Sci. 162:632–640.

Moldrup, P., T. Olesen, T. Yamaguchi, P. Schjonning, and D. Rolston. 1999. Modeling diffusion and reaction in soils: IX. The Buckingham-Burdine-Campbell equation for gas diffusivity in undisturbed soil. Soil Sci. 164:542–551.

Mosier, A. R., W. J. Parton, and G. L. Hutchinson. 1983. Modelling nitrous oxide evolution from cropped and native soils. Environ. Biochem. 35: 229–241.

Mosier, A., C. Kroeze, C. Nevison, O. Oenema, S. Seitzinger, and O. Van Cleemput. 1998. Closing the global $N_2O$ budget: Nitrous oxide emissions through the agricultural nitrogen cycle. Nutr. Cycling Agroecosyst. 52:225–248.

Mosier, A., J. Duxbury, J. Freney, O. Heinemeyer, and K. Minami. 1996. Nitrous oxide emissions from agricultural fields: Assessment, measurement and mitigation. Plant and Soil. 181:95–108.

Parton, W., A. Mosier, D. Ojima, D. Valentine, D. Schimel, K. Weier, and A. Kulmala. 1996. Generalized model for $N_2$ and $N_2O$ production from ni-

trification and denitrification. Global Biogeochem. Cycles 10:401–412.

Pauling, L. 1970. General Chemistry. Dover, New York.

Pires, M., M. Rossi, and D. Ross. 1994. Kinetic and mechanistic aspects of the NO oxidation by $O_2$. in aqueous phase. Intl. J. Chem. Kinet. 26: 1207–1227.

Remde, A., F. Slemr, and R. Conrad. 1989. Microbial production and uptake of nitric oxide in soil. FEMS Microbiol. Ecol. 62:221–230.

Reuss, J., and R. Smith. 1965. Chemical reactions of nitrites in acid soils. Soil Sci. Soc. Am. Proc. 29:267–270.

Riley, W., and P. Matson. 2000. NLOSS: A mechanistic model of denitrified $N_2O$ and $N_2$ evolution from soil. Soil Sci. 165:237–249.

Rudolph, J., and R. Conrad. 1996. Flux between soil and atmosphere, vertical concentration profiles in soil, and turnover of nitric oxide: 2. Experiments with naturally layered soil cores. J. Atmos. Chem. 23:275–300.

Rudolph, J., F. Rothfuss, and R. Conrad. 1996. Flux between soil and atmosphere, vertical concentration profiles in soil, and turnover of nitric oxide: 1. Measurements on a model soil core. J. Atmos. Chem. 23:253–273.

Skiba, U., K. Hargreaves, D. Fowler, and K. Smith. 1992. Fluxes of nitric and nitrous oxides from agricultural soils in a cool temperate climate. Atmos. Environ. 26A:2477–2488.

Stevenson, F., and R. Swaby. 1964. Nitrosation of soil organic matter: I. Nature of gases evolved during nitrous acid treatment of lignins and humic substances. Soil Sci. Soc. Am. Proc. 28:773–778.

Thorn, K., and M. Mikita. 2000. Nitrite fixation by humic substances: Nitrogen-15 nuclear magnetic resonance evidence for potential intermediates in chemodenitrification. Soil Sci. Soc. Am. J. 64:568–582.

Van Cleemput, O., and L. Baert. 1976. Theoretical considerations on nitrite self-decomposition reactions in soils. Soil Sci. Soc. Am. J. 40:322–324.

Van Cleemput, O., and L. Baert. 1984. Nitrite: A key compound in N loss processes under acid conditions? Plant Soil 76:233–241.

Venterea, R., and D. Rolston. 2000a. Mechanisms and kinetics of nitric and nitrous oxide production during nitrification in agricultural soil. Global Change Biol. 6:1–14.

Venterea, R., and D. Rolston. 2000b. Mechanistic modeling of nitrite accumulation and nitrogen oxide gas emissions during nitrification. J. Environ. Qual. 29:1741–1751.

Venterea, R., and D. Rolston. 2000c. Nitric and nitrous oxide emissions following fertilizer application to agricultural soil: Biotic and abiotic mechanisms and kinetics. J. Geophys. Res.-Atmos. 105(D12):15., 117–15,129.

Venterea, R., and D. Rolston. 2002. Nitrogen oxide trace gas transport and transformation: I. Evaluation of data from intact soil cores. Soil Sci. 167: 35–48.

Whitaker, S. 1988: The use of assumptions, restrictions and constraints in engineering analysis. Chem. Eng. Educ. Spring:104–108.

Williams, E., D. Parrish, and F. Fehsenfeld. 1987. Determination of nitrogen oxide emissions from soils: Results from a grassland site in Colorado, United States. J. Geophys. Res.-Atm. 92:2173–2179.